applied sciences

MDPI

Article

Triangular Position Multi-Bolt Layout Structure Optimization

Xiaohan Lu [1], Min Zhu [1,*], Yilong Liu [1], Shengao Wang [1], Zijian Xu [1] and Shengnan Li [2]

1 College of Nuclear Science and Technology, Naval University of Engineering, Wuhan 430030, China
2 College of Power Engineering, Naval University of Engineering, Wuhan 430030, China
* Correspondence: min0zhu@163.com; Tel.: +86-13505358526

Abstract: Stress concentration often occurs around bolt holes in load-bearing joint structures of large complex equipment, ships, aerospace and other complex machinery fields, which is an important mechanical factor leading to the failure of joint structures. It is of great engineering significance to study the phenomenon of stress concentration on connected structures for the safety of large and complex equipment; meanwhile, the layout of bolts seriously affects the stress around holes. Many scholars have studied the layout optimization of multi-bolted structures through experiments and simulations, but few algorithms have been applied to the layout optimization of bolted structures. And most of the studied types of multi-bolt structures are symmetrical. Therefore, in this paper, the gray wolf algorithm is used to optimize the layout of nickel steel plate connectors with a bolt layout in triangular position, and the optimal objective function is found based on the hole circumferential stress of the nickel steel plate, maximum shear stress of the bolt and bending stress of the nickel steel plate. Comparing the optimal values obtained by the fruit fly optimization algorithm, particle swarm optimization algorithm, gray wolf optimization algorithm, multiverse optimization algorithm and wind driven optimization algorithm, the accuracy of selecting the gray wolf algorithm for optimization is verified. A multi-bolt connection structure model was established in ABAQUS, and the surface stress before and after optimization was compared to verify the correctness of the gray wolf algorithm applied to the structure layout optimization of the nickel steel flat bolt connection. The results show that under the force of 15 KN, compared with the original bolt structure layout, the optimized upper side nickel steel plate bore peripheral stress is reduced by 73.1 MPa, and the optimization rate is 24%; bolt stress is reduced by 47.7 MPa, and the optimization rate is 12.5%; when the load is less than 18 KN, the optimization effect of both the upper nickel steel plate and bolt group is more than 10%. When the load is greater than 18 KN, the optimization effect is reduced, and when the load is greater than 21 KN, the nickel steel plate has exceeded the yield limit. Due to the existence of fixed constraints, the optimization of the lower nickel steel plate is not obvious. The results of this study can provide data and theoretical support for the layout optimization of the nickel steel flat bolt connection structure, and help to improve reliability analysis and health monitoring in complex assembly fields such as large complex equipment and aerospace.

Keywords: bolted connection; layout optimization; algorithm; ABAQUS

Citation: Lu, X.; Zhu, M.; Liu, Y.; Wang, S.; Xu, Z.; Li, S. Triangular Position Multi-Bolt Layout Structure Optimization. *Appl. Sci.* **2023**, *13*, 8786. https://doi.org/10.3390/app13158786

Academic Editors: Phong B Dao, Lei Qiu, Liang Yu, Tadeusz Uhl and Minh-Quy Le

Received: 10 June 2023
Revised: 18 July 2023
Accepted: 24 July 2023
Published: 29 July 2023

1. Introduction

A bolted connection is an important connection method in large complex equipment, aerospace and other mechanical structures [1–3]. The service life of the bolt and normal operation of the mechanical structure are directly affected by the change in the preload force of the connection mode. The stress around the hole of the bolted connection is the key point that affects the construction life. In order to make the structure more stable and reduce the stress on the bearing structure, it is necessary to optimize the layout of the multi-bolt connection structure to achieve a better connection effect. Many scholars have carried out a lot of research on the optimization of bolt layout.

The stress distribution of the bolt-connected structure is affected by the thickness of the cover plate, aperture, nut diameter and other factors. When the value of the aperture and nut diameter is small, the stability of the bolt-connected structure can be improved [4]. Liu et al. [5] tested the mechanical properties of asymmetrical bolts and came to the conclusion that the performance of the copper gasket is stable and bearing capacity is higher than that of an aluminum gasket. Moreover, under the action of a copper gasket, the coefficient of friction imbalance is between 0.919 and 1.050, which can show good slip and energy dissipation under earthquake conditions.

It takes time and effort to study the effect of bolt layout on the mechanical properties of the connected structure by experiment, so many researchers optimize and analyze the performance of the bolted structure by the simulation method. Wu et al. [6] used a parametric model to adjust the layout of the bolt connection plate by changing the radius and angle of the bolt connection, and then analyzed its influence on the modal frequency. The results show that there are some order mode frequencies that affect the bolt layout, and these frequencies should be avoided. Pedersen [7] optimized the shape of the starting point and root of the thread, and also optimized the bolt rod and thread, which reduced the stress by 34%, reduced the stiffness of the bolt, increased the stiffness of the bolt connection and greatly extended the fatigue life.

In order to simulate the bolted structure more accurately, more and more scholars apply artificial intelligence to the simulation. Shen et al. [8] improved the genetic algorithm, applied the improved objective function to the connection structure, took the average acceleration at the corner of the component as the objective function of the algorithm, adopted the idea of parametric modeling, realized the interaction between MATLAB and NASTRAN, and reduced the stress value at the corner of the component. The layout of the bolt on the edge of the component is optimized and the safety of the component is improved. Han et al. [9] used the gray wolf algorithm to optimize the motion trajectory of each joint of the robotic arm, which takes time efficiency and smoothness as the objective function, and the results show that the gray wolf algorithm can effectively perform trajectory optimization. Liang et al. [10] improved the thresholds and weights of an Elman neural network by particle swarm algorithm and applied the method to clock difference forecasting, which can improve the stability and forecasting accuracy of a satellite clock. Wang et al. [11] carried out layout optimization experiments on bolt sets based on the firefly algorithm, and carried out simulation analysis on double-row bolts and three-row bolts, and the optimized bolt layout reduced the perimeter stress of the holes and improved the safety of the structure. However, the optimization of multi-bolt joint structures in the existing literature is limited to symmetric bolt structures [12–16], while there are few studies on asymmetric bolt structures, especially the optimization of a multi-bolt layout in a triangular position. In addition, researchers rarely apply the gray wolf optimization algorithm to the layout optimization of the connection structure of large complex equipment. Therefore, based on the gray wolf algorithm, this paper optimizes the bolt group of the triangular multi-bolt layout structure, seeks the optimal bolt margin and spacing, and reduces the surface stress of the connection structure and maximum stress on the surface of the bolt group; to prevent excessive stress around the bolt hole, resulting in fatigue damage of the bolt hole or plastic deformation of the connector, thus affecting the stability and reliability of the connection. Nickel steel has the advantages of strong compressive resistance, corrosion resistance, low temperature toughness and so on, and is widely used in aerospace and other large complex important equipment, and there is little research on nickel steel. Therefore, the connection structure of this paper chooses nickel steel.

Based on the above background, this paper analyzes the hole surrounding stress, maximum shear stress of the bolt and bending stress of the nickel steel plate; and adopts the gray wolf algorithm to optimize the bolt spacing and bolt diameter, which can accurately find the optimal bolt spacing and bolt radius. The results of the fruit fly optimization algorithm [17], particle swarm optimization algorithm [18], gray wolf optimization algorithm [19], multiverse optimization algorithm [20] and wind driven optimization algorithm [21] for triangular multi-bolt layout structure optimization were compared, and the accuracy of the gray wolf optimization algorithm was verified. The optimized bolts still met the requirements of the design specification, and the efficiency of the joint design is improved. ABAQUS-2022 software was used to establish the finite element model of the optimal solution, and the stress conditions of the nickel steel plate and bolts before and after optimization were compared to verify the correctness of the algorithm, objective function and constraint conditions. Based on the gray wolf algorithm, this paper selects the optimal triangular multi-bolt layout structure and corresponding bolt diameter, and reduces the hole stress and maximum stress on the surface of the nickel steel plate, which provides a new idea for the layout optimization of the asymmetric bolt-connected structure, improves the strength and stiffness of the structure, and extends the service life and reliability of the bolt-connected structure. When engineering design bolts and connecting structures, the optimal solution of the gray wolf algorithm can select a reasonable range of bolt diameters and bolt spacing, so that the stress around bolt holes is within a reasonable range, avoiding excessive use of materials and reducing material costs. It is helpful to improve the safety and reliability of load-bearing connection structures in complex machinery fields such as large complex equipment, ship sailing and aerospace.

2. Materials and Methods

2.1. Principles of the Grey Wolf Algorithm

2.1.1. Algorithm Introduction

The gray wolf algorithm is designed based on the hunting system and leadership level of the gray wolf [22]. The pyramid level of the algorithm is divided into four layers. The top gray wolf is responsible for decision-making events such as hunting and distribution of goods, called α. The second layer is the top gray wolf's think tank team, called β. It is mainly responsible for assisting in decision-making, and when the top position is vacant, the second layer of workers will take over the top position. The third layer of workers, called δ, listens to the transfer orders of the first two layers and is mainly responsible for tasks such as nursing and sentinel. The bottom worker, known as ω, mainly works to balance internal relationships.

The gray wolf algorithm has fast convergence speed, has high global search ability, can be applied in different problem domains, does not require complex computer models, and can automatically adapt to the characteristics of the problem and change of search space. To sum up, the gray wolf algorithm is selected in this paper to optimize the layout of the multi-bolt connection structure.

2.1.2. Round up Prey

The prey catching behavior of the gray wolf group is defined as [19]:

$$\vec{D} = \left| \vec{C}\vec{X}_p(t) - \vec{X}(t) \right| \tag{1}$$

$$\vec{X}(t+1) = \vec{X}_p(t) - \vec{A}\vec{D} \tag{2}$$

Formula (1) is the distance between the gray wolf and its prey, and Formula (2) is the formula for updating the position of the gray wolf. Where, t represents the current number of iterations, $\vec{A}$ and $\vec{C}$ are the position vector of the prey and the position vector of the gray wolf, respectively. $\vec{X}_p$ and $\vec{X}$ are the coefficient vector. The formula for calculating $\vec{A}$ and $\vec{C}$ are as follows [19]:

$$\vec{A} = 2\vec{a}\vec{r}_1 - \vec{a} \tag{3}$$

$$\vec{C} = 2\vec{r}_2 \tag{4}$$

where, $\vec{a}$ is the convergence factor, *r*ß1 and *r*ß2 are the random number between the interval [0–1].

2.1.3. Hunt

Grey wolves can identify the specific location of prey by themselves [23], and under the leadership of the gray wolves at the top of the pyramid, gradually surround the prey, so that each gray wolf can reach the best position. Therefore, in order to simulate the behavior of the gray wolf, we selected three optimal positions around the prey, used these three positions to judge the specific position of the prey, and forced other gray wolves to update their own positions according to the position of the optimal gray wolf. By closing in on the prey, they round it up. The principle of gray wolf individual location renewal is shown in Figure 1.

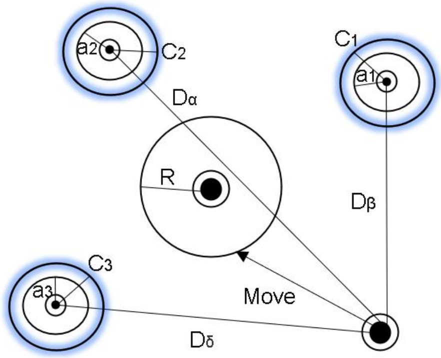

Figure 1. Schematic diagram of individual renewal position of a gray wolf.

Its mathematical model is described as follows [19]:

$$\begin{cases} \vec{D}_\alpha = \left|\vec{C}_1\vec{X}_\alpha - \vec{X}\right| \\ \vec{D}_\beta = \left|\vec{C}_2\vec{X}_\beta - \vec{X}\right| \\ \vec{D}_\delta = \left|\vec{C}_3\vec{X}_\delta - \vec{X}\right| \end{cases} \tag{5}$$

$\vec{D}_\alpha$,$\vec{D}_\beta$,$\vec{D}_\delta$ are the distance vector between α, β, δ and other gray wolves, $\vec{X}_\alpha$, $\vec{X}_\beta$, $\vec{X}_\delta$ are the vector of the former position of α, β, δ, $\vec{C}_1$, $\vec{C}_2$, $\vec{C}_3$ are the random vector, $\vec{X}$ represents the current position vector.

$$\begin{cases} \vec{X}_1 = \vec{X}_\alpha - A_1\vec{D}_\alpha \\ \vec{X}_2 = \vec{X}_\beta - A_2\vec{D}_\beta \\ \vec{X}_3 = \vec{X}_\delta - A_3\vec{D}_\delta \end{cases} \tag{6}$$

Formula (6) shows the direction and step length of an individual gray wolf ω moving toward α, β, δ respectively.

$$\vec{X}(t+1) = \frac{\vec{X}_1 + \vec{X}_2 + \vec{X}_3}{3} \tag{7}$$

Formula (7) is the optimal position of the bottom gray wolf ω.

2.1.4. Attack Prey

To simulate the movement of gray wolves as they approach prey, as $\vec{a}$ decreases, the range of $\vec{A}$ decreases, the value interval of $\vec{A}$ is $[-\alpha, \alpha]$. When $\vec{A}$ is located in this interval, the gray wolf can switch between its own position and the position of prey at will. When $|\vec{A}| < 1$, the gray wolf pack attacks and captures its prey.

2.2. Construct Objective Function

2.2.1. Bolt Mechanical Model

Apply a pull in the positive direction of X and a pull in the negative direction of Y at point K, both of which are 15 KN. Among them, the bolts are arranged in the position of an equilateral triangle, whose side length is a and centroid is O. The structural diagram is shown in Figure 2.

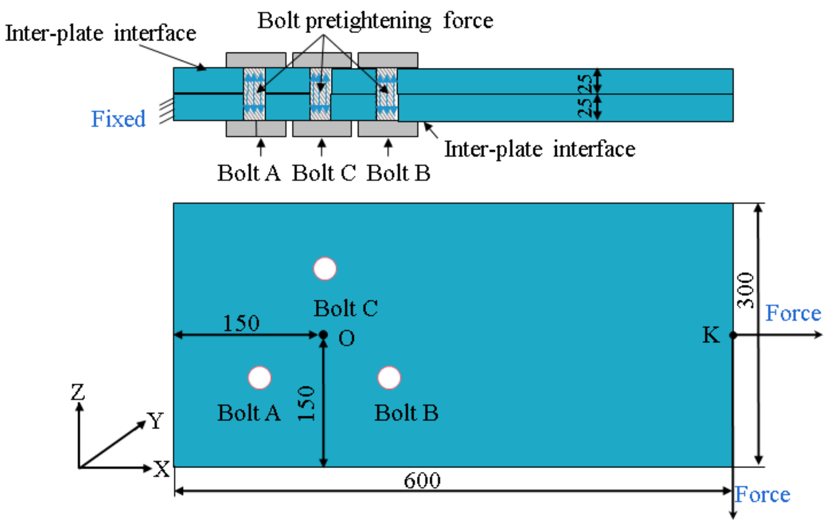

Figure 2. Schematic diagram of bolt structure.

By simplifying the force at point K to point O, the torque at point O is formed. Carrying out force analysis on bolts A, B and C:

$$F_A = \left(5 - \frac{2250\sqrt{3} \times \sin 30^o}{a}\right)\vec{i} + (-5 - \frac{2250\sqrt{3} \times \cos 30^o}{a})\vec{j} \tag{8}$$

$$F_B = \left(5 - \frac{2250\sqrt{3} \times \cos 30^o}{a}\right)\vec{i} + (-5 + \frac{2250\sqrt{3} \times \sin 30^o}{a})\vec{j} \tag{9}$$

$$F_C = \left(5 + \frac{2250\sqrt{3}}{a}\right)\vec{i} + (-5)\vec{j} \tag{10}$$

According to Equations (8)–(10), from F_A, F_B and F_C, it can be seen that the maximum force is bolt C:

$$F_{max} = F_C \tag{11}$$

At this time, the maximum shear stress on the bolt is:

$$\tau_{max} = \frac{F_{max}}{\pi d^2/4} \tag{12}$$

It can be seen from the analysis that bolt B receives the maximum torque. Bolt B is cut along the Y-axis to obtain the profile as shown in Figure 3a and the torque diagram of the plate as shown in Figure 3b.

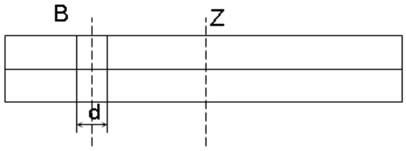

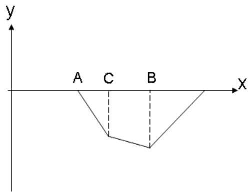

Figure 3. Bolt profile and torque diagram. (**a**) Profile of the nickel steel plate; (**b**) Torque diagram of nickel steel plate.

The torque and moment of inertia at bolt B are:

$$M = F_B\left[300 + (150 - \frac{a}{2})\right] \quad (13)$$

$$I = I_{max} - \left[I_{hole} + I_{offset}\right] = \frac{10 \times 300^3}{12} - \left[\frac{10d^3}{12} + \left(\frac{a}{2\sqrt{3}}\right)^2 \times 25\text{d}\right] \quad (14)$$

Then the critical bending stress of the nickel steel plate is:

$$\sigma_{max} = \frac{M}{I} \quad (15)$$

Formulas (11), (12) and (15) can be used to calculate the maximum stress on bolts, maximum shear stress and critical bending stress of the nickel steel plate, which lays a prerequisite for the selection of the objective function in the following algorithm.

2.2.2. Objective Function

In this paper, the simulation software ABAQUS was used to simulate the working condition of bolts [24], and the maximum stress, maximum shear stress and critical bending stress of bolts were considered at the same time [25]. In order to fit the three objective functions into one objective function, their superposition was processed:

$$Fitness = Fmax + \frac{4 \times Fmax}{\pi {x_2}^2} + \frac{6 \times F_B \times (450 - \frac{x_1}{2})}{1.35 \times 10^8 - (5{x_2}^3 + 45{x_1}^2 x_2)} + k(x_1, x_2) \quad (16)$$

where, x_1 is the distance variable a between bolts; x_2 is the diameter d of the bolt; $k(x_1, x_2)$ is the fitting factor added when fitting $F_{max}, \tau_{max}, \sigma_{max}$.

2.3. Selection Constraint

Before the algorithm is solved, the population number pop is set to 50, variable dimension dim is 2, maximum number of iterations maxIter is 500, upper boundary velocity is [2, 2] and lower boundary velocity is [−2, −2]. For M8-type bolts, the distance between the bolts and nickel steel plate, and distance between the bolts cannot be too small; according to the steel design code [26], the distance between its bolts is not less than 3d and the end distance of the bolts is not less than 1.5d. Also considering the diameter of small bolts, the variation range of the bolt diameter d is [1.4~36]. Therefore, the range of spacing a and bolt diameter d selected in this paper is:

2.8 mm < a < 142.5 mm

1.4 mm < d <3 6 mm

2.4. Finite Element Modeling and Boundary Conditions

The bolt specifications in this paper refer to GB/T191-197-2003 [27], and M8 bolts with a pitch of 1.25 mm and a screw length of 50 mm are selected. Nickel steel has important properties such as formability, weldability and ductility, and has good corrosion resistance. It is an important material, and widely used in large equipment, aerospace and other complex assemblies in the field of connection structures. At present, there is little research in the field of nickel steel plates, so the bolt role of the plate in this paper is selected from nickel steel material. The modulus of elasticity of both the bolt and nickel steel plate is 210,000 MPa, the Poisson's ratio is 0.283 and the density is 7999 kg$\cdot$m^{-3}; the maximum stress limit of the bolt is 640 MPa and maximum stress limit of the nickel steel plate is 340 MPa.

To verify the accuracy of the objective function as well as the algorithm, parametric modeling of the bolt and nickel steel flat plate was carried out based on ABAQUS with Python-3.90 software. Due to the difficulty of meshing the threads in ABAQUS and non-convergence of the calculations, the paper uses a simplified modeling of the bolts without threads [28] and makes the multi-bolt structure act on the bearing surface by applying a preload [29]. The load-bearing structure is two thin nickel steel plates, both of which are elastoplastic flat plates. The two fast nickel steel flat plates were superimposed to simulate the connecting action of complex equipment, as shown in Figure 4. The nickel steel plate is meshed using a hexahedral structured mesh with a cell type of C3D8R cells. In order to make the simulation easier to converge and more precise, the area around the bolt holes and nut of the nickel steel plate is divided to obtain a more precise mesh, as shown in Figure 5 below.

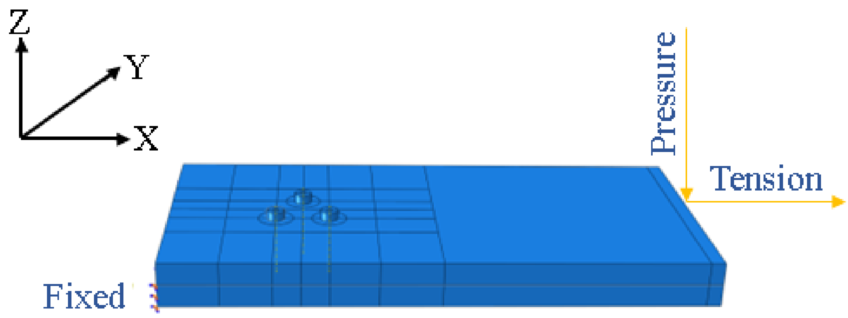

Figure 4. Bolted connection model.

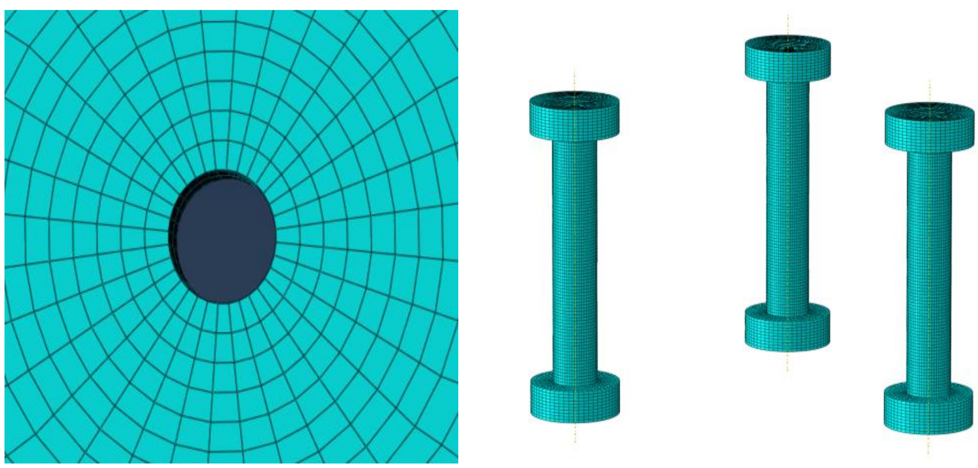

Figure 5. Stress of multiple bolts.

In this paper, a high quality mesh with 45,430 meshes is divided and partitioned at different locations to ensure the accuracy of the calculation results. At the same time, the finite element analysis method has been widely used in the simulation analysis of the model, and the reliability of its analysis results can be effectively guaranteed under the condition of ensuring high quality meshes.

In the solution stage, this paper sets four analysis steps, the first and second steps in the bolt's middle surface, gradually add the bolt load, that is, the preload. In the third and fourth steps, the current length is fixed in order to meet the actual engineering requirements, so that the bolt load changes with the deformation of the structure.

The contact properties are set to finite slip and the junction-surface discretization method is used. For contact, the harder nickel steel plate is used as the master surface and the bolt surface as the slave surface, defaulting to contact when the distance between the two is less than 0.03. The tangential contact is set with a friction coefficient of 0.3, and the normal contact is a hard contact to prevent penetration.

If a force of 15 KN is applied in the X and Y directions, the bolt will be severely deformed, thus affecting the simulation results, and the simulation mainly compares the stresses on the nickel steel plate and bolt before and after optimization, independent of the force direction of the plate. Therefore, in Step 3, the tension and pressure are applied to the upper nickel plate in the positive X-axis and negative Z-axis directions. The leftmost side of the lower nickel steel board applies a fixed restraint.

3. Results

3.1. Algorithm Solution

Based on the MATLAB(2020) software for the multi-bolt connection structure of the spacing a and diameter d of the bolt to find the best calculation, from Figure 6, it can be seen that the objective function and constraints are fully applicable to the gray wolf algorithm program, the iterative effect is good, and finally stable convergence to a fixed value is observed. Its convergence to a stable fitness value is not used as a criterion for judging bolts and nickel steel plates. As can be seen from Figure 7, through different iterations, the particles gradually converge to the best particle, whose best particle is the result sought. The algorithm results in a pitch a = 108.5629 mm and a diameter d = 9.0233 mm. The results optimized by firefly algorithm for the spacing of double-row bolts and triple-row bolts in previous studies [11] are not much different from the optimized bolt spacing in this paper, and are also consistent with the results optimized by Xiao et al. [30] for the layout optimization of bolt groups for flameproof boxes used in mines.

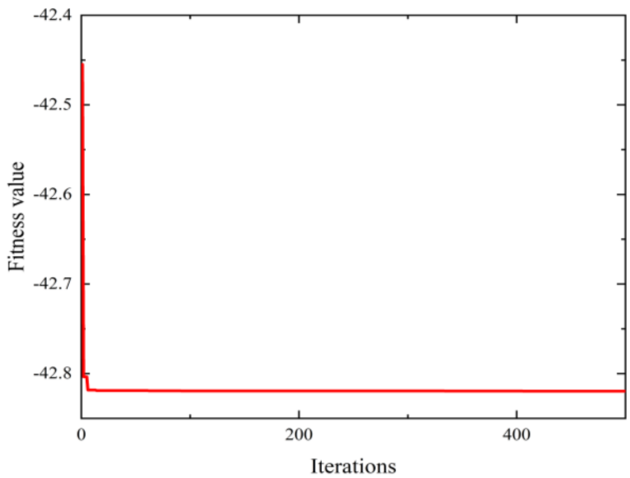

Figure 6. Results of algorithm operation.

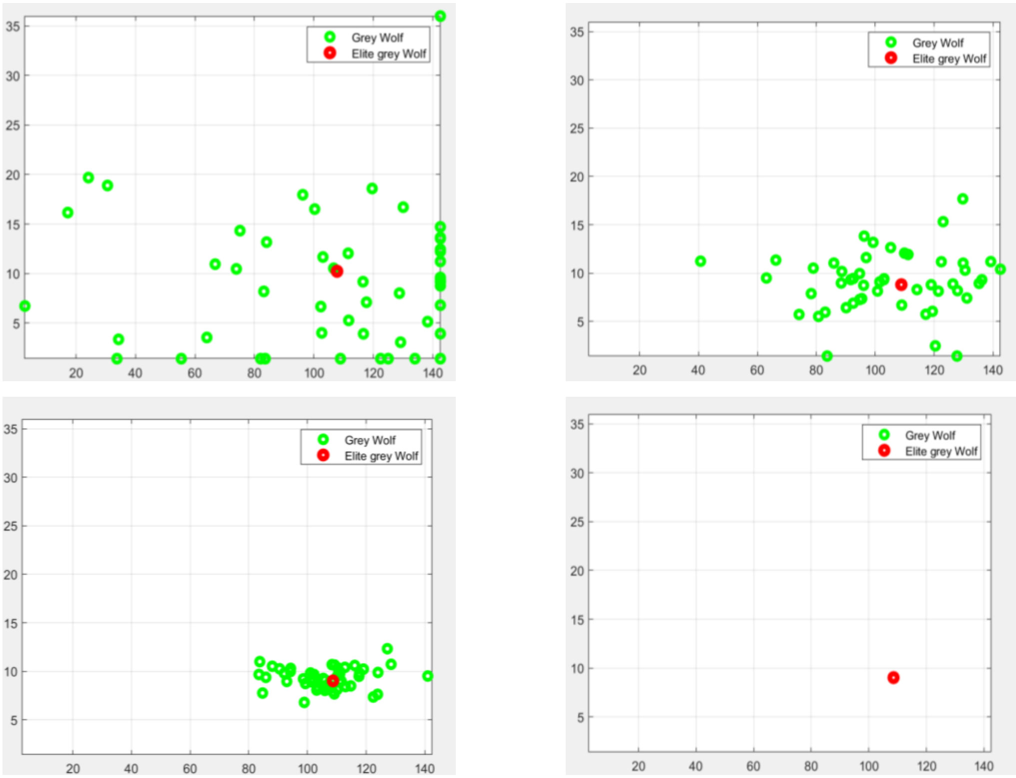

Figure 7. Different iteration times of the algorithm.

In this paper, the objective function as well as the boundary conditions are applied to the fruit fly optimization algorithm, particle swarm optimization algorithm, gray wolf optimization algorithm, multiverse optimization algorithm and wind driven optimization algorithm, the results of which are shown in Figure 8, with approximately the same algorithmic optimization curves. There is only a slight difference at the initial iteration, which is explained by the fact that the different algorithms contain different principles. As shown in Table 1, the final fitness values were all stable at −42.8195, with the gray wolf algorithm having the highest number of iterations, but none of them exceeded 500 iterations.

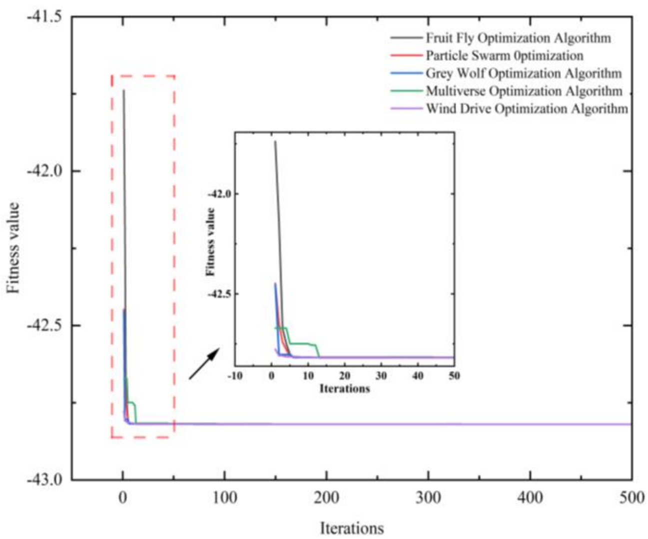

Figure 8. Optimization effects of different algorithms.

Table 1. The number of fastest iterations.

Algorithm	Fastest Iteration (Generation)	Stable Value
Fruit Fly Optimization Algorithm	70	−42.8195
Particle Swarm Optimization	77	−42.8195
Gray Wolf Optimization Algorithm	342	−42.8195
Multiverse Optimization Algorithm	315	−42.8195
Wind Driven Optimization Algorithm	150	−42.8195

Figure 9 shows the optimal result values calculated by various algorithms, and the results calculated by the particle swarm optimization algorithm, multiverse algorithm and gray wolf algorithm are roughly the same. The bolt spacing and bolt diameter calculated by the fruit fly optimization algorithm are both larger, while the bolt spacing and bolt diameter calculated by the wind driven optimization algorithm are larger and smaller. Because the core functions of various algorithms are different, there is a certain deviation, which is also a limitation of artificial intelligence. In this simulation, the maximum deviation of the bolt diameter is 0.59% and maximum deviation rate of bolt spacing is 0.12%, both of which have small deviations and can be ignored. The results show that the optimal solutions of the five algorithms selected in this paper are roughly the same, and the deviation rate is low, which will not cause certain impact on the subsequent simulation analysis. Therefore, this paper can choose the optimal solution calculated by the gray wolf optimization algorithm as the focus of the subsequent analysis and discussion.

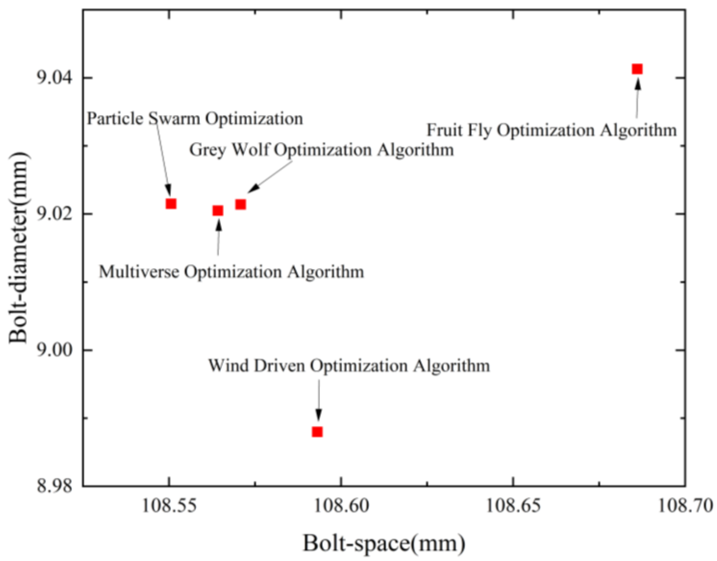

Figure 9. Algorithm optimization results.

3.2. Optimized Stress Comparison between Front and Rear Bolts

The ABAQUS-based simulation design can verify the correctness of the optimal solution selection of the gray wolf algorithm to reduce the stress concentration phenomenon in the structure and thus improve the safety performance of the aerostructure. The stress clouds of the upper nickel steel plate, lower nickel steel plate and bolts before and after optimization are shown in Figures 10–12.

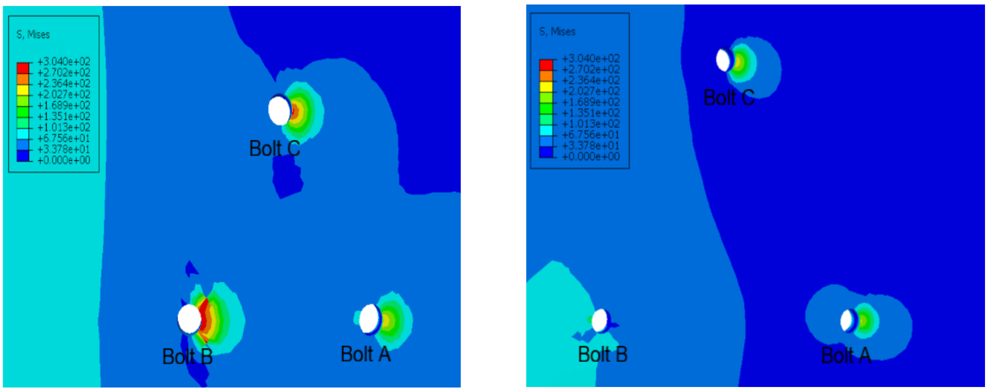

(a) (b)

Figure 10. Upper nickel steel plate stress cloud. (**a**) Optimized pre-stress nephogram; (**b**) Optimized stress nephogram.

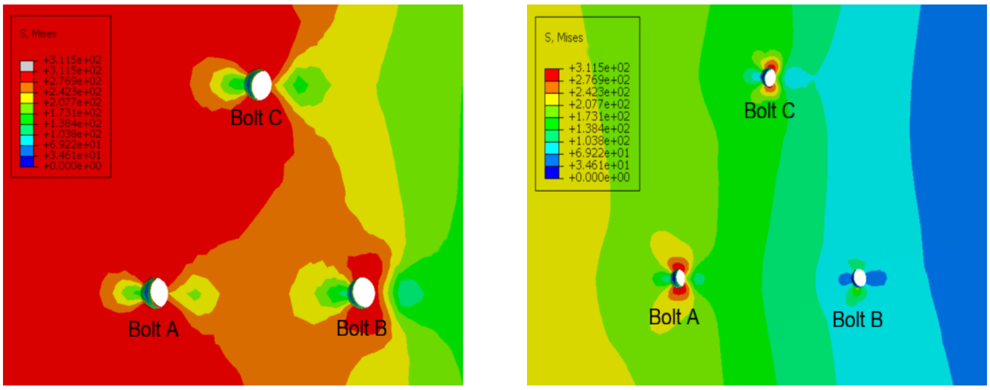

(a) (b)

Figure 11. Lower nickel steel plate stress cloud. (**a**) Optimized pre-stress nephogram; (**b**) Optimized stress nephogram.

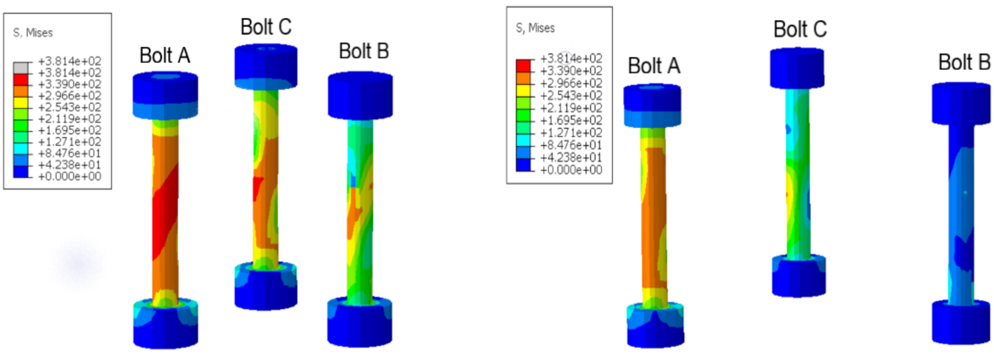

(a) (b)

Figure 12. Stress clouds for bolt sets in triangular positions. (**a**) Optimized pre-stress nephogram; (**b**) Optimized stress nephogram.

The stress cloud diagram of the nickel steel plate above is shown in Figure 10. In order to make the stress nephogram visually compare the stress change and stress concentration through images, this paper takes the stress extreme value before optimization as the standard and changes the mechanism of the optimized nephogram. Before and after optimization, the maximum stress of the nickel steel plate is 304.0 MPa and 230.9 MPa, respectively, and the maximum stress is reduced by 73.1 MPa, with an optimization rate of 24%. A previous study [8] optimized the layout of the bolts on the connection structure based on the improved genetic algorithm, and the results showed that the optimized bolt layout reduces the maximum equivalent stress at corners constructed by 20.4%. In another study [11], the firefly algorithm was used to optimize bolts with double and triple rows, and the results showed that after optimization, the stress around the hole of the plate structure with triple rows of bolts was reduced by about 20%, and the stress reduction effect in this paper was better. Xiao et al. [31] adopted the improved genetic algorithm to optimize the equivalent stress of the aviation connection structure under the position of three rows of bolts under severe working conditions. The results showed that the maximum pore circumference stress was reduced by 31.03% under a static pressure load of 30 MPa, while the optimization efficiency only reached 23.36% under severe working conditions. Under the conditions of 15 KN tension and pressure studied in this paper, it is already a serious condition, and the optimization effect of both is the same, which proves the reliability and accuracy of the analysis in this paper. Among them, the stress around bolt hole B decreased significantly after optimization, and the maximum stress value around bolt hole B decreased from 304.0 MPa to 112.1 MPa, with a decrease rate of 63.1%, which greatly reduced the stress around bolt hole B. The stress around bolt hole C before and after optimization is 309.2 MPa and 302.8 MPa, respectively. Bolt hole C was originally the most stressed bolt, and its optimization effect is not obvious. The stress around bolt hole A is increased by 27.9 MPa, mainly because after optimization, the position of bolt hole A is closer to the edge of the nickel steel plate, and the position of concentrated force is closer to the vicinity of bolt A.

Figure 11 shows the stress cloud map of the lower nickel steel plate. Before and after optimization, the maximum stress of the nickel steel plate is 311.5 MPa and 302.8 MPa, respectively, and the maximum stress is reduced by 8.7 MPa, with an optimization rate of 2.8%. The maximum stress at bolt hole B decreased from 307.1 MPa to 177.5 MPa, and the optimization rate was 42.2%, which significantly improved the stress concentration phenomenon at bolt hole B. The maximum stress at bolt holes A and C decreased less, 8.9 MPa and 6.4 MPa, respectively, but the equivalent stress around them decreased significantly. According to the stress nephogram, the stress concentration around the three bolt holes has been significantly improved after the optimization of the triangular multi-bolt connection structure, and the bolt hole B has been greatly improved.

Figure 12 shows that before and after the optimization, the stresses on bolt A were 381.4 MPa and 333.7 MPa, respectively, both of which were the maximum values of the bolt stresses before and after the optimization, and the maximum stress was reduced by 47.7 MPa, and its optimization rate was 12.5%. The literature [31] applied the improved genetic algorithm to the layout optimization of an actual aerospace bolt connection structure, and the results showed that the maximum equivalent stress of the bolt was reduced by 10.14%, which is not much different from the results of this paper. The main reason for the highest stress value in bolt A is the left-hand fixation of the nickel steel plate below, which affects the forces in the connection structure. Bolt B has the most obvious optimization effect, with its maximum equivalent force dropping by 177.5 MPa and optimization rate of 57.2%, effectively extending the service life and reliability of bolt B. The maximum stress value at bolt C was reduced from 345.5 MPa to 301.0 MPa, with an optimization rate of 12.9%. In summary, the bolts in the triangular position were improved by the optimal solution calculated by the gray wolf algorithm, which improved the overall safety and stability. In the literature [32], the layout of the beam-column extended end-plate connection structure was optimized based on the firefly algorithm, and the maximum hole perimeter equivalent force of the connection structure was reduced by 41.2 MPa after optimization, with an optimization rate of 10.9%; however, the maximum equivalent force on its bolt surface was reduced by only 3.8%. Compared with this paper, which uses the gray wolf algorithm to optimize the multi-bolt layout in triangular positions, this method is more efficient and can provide an effective reference for engineers when designing multi-bolt connection structures for nickel steel flat plates.

Before and after the optimization, the stress concentration around the hole of the nickel steel plate is improved, especially the maximum stress at the bolt hole B, which reaches 40–60% of the optimized value. The overall optimization rate for the upper nickel steel plate is 24% and the overall optimization rate for the lower nickel steel plate is 2.8%, mainly due to the fixed restraint applied on the left side. The overall optimization rate for the bolt set was 12.5%.

In order to study the optimization under different force conditions, this paper changed the pressure and tension and added comparative analysis, respectively, 3 KN, 9 KN, 15 KN and 21 KN, as shown in Figure 13. The results show that under the 18 KN load, the nickel steel plate and bolt set above can achieve better optimization efficiency, and their optimization rates are above 10%. At 15 KN, the optimization effect is better. However, when the load is greater than 18 KN, the optimization efficiency is lower. When the load is greater than 21 KN, the nickel steel plate has exceeded the yield limit and presents a large deformation condition, which is not suitable for calculating its optimization efficiency. The optimization efficiency of the lower nickel steel plate is always lower, mainly because of the fixed constraints on the lower nickel steel plate. Overall, the analysis of this paper proves that the gray wolf algorithm is suitable for structural optimization of multi-bolt layouts in triangular positions, which helps to reduce the stress concentration phenomenon and contributes to the effective structural optimization design of large and complex equipment and aeronautical structures.

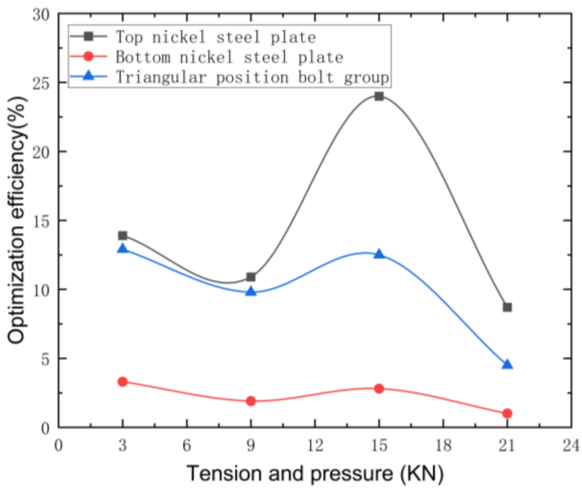

Figure 13. Comparison chart for optimisation of different force cases.

4. Conclusions

This paper applies the gray wolf algorithm to optimize the structural layout of multi-bolt positioning in triangular configurations. By analyzing the forces, the objective function is formulated based on the fitted functions of hole perimeter stress for nickel steel plates, maximum shear stress for bolts and bending stress for nickel steel plates. The value range for bolt diameter and spacing is determined according to design specifications. The optimal solutions calculated using the fruit fly optimization algorithm, particle swarm optimization algorithm, gray wolf optimization algorithm, multi-verse optimization algorithm and wind driven optimization algorithm are compared. ABAQUS simulation software is used to model and compare the stress on nickel steel plates and bolts before and after optimization, thereby verifying the correctness of the algorithm application. Through analysis, the following conclusions can be drawn:

(1) Before optimization, a traditional design method was used with a bolt spacing of 60 mm and a bolt diameter of 8 mm. After optimization, the bolt spacing is chosen as 108.5629 mm and bolt diameter is 9.0233 mm. The stress distribution of the newly

arranged nickel steel plate is more uniform, and the local stress values have also been reduced, resulting in a more stable overall stress state.

(2) Through this layout optimization, under pressures and tensions of 15 KN, the hole perimeter stress on the upper nickel steel plate decreased by 73.1 MPa, with an optimization rate of 24%. The hole perimeter stress on the lower nickel steel plate decreased by 8.7 MPa, with an optimization rate of 2.8%. The maximum equivalent stress on the bolts decreased by 47.7 MPa, with an optimization rate of 12.5%.

(3) When the load is less than 18 KN, the optimization effect of both the upper nickel steel plate and bolt assembly is above 10%. However, when the load exceeds 18 KN, the optimization effect decreases. When the load exceeds 21 KN, the nickel steel plate has exceeded its yield limit. The upper nickel steel plate shows significant optimization, but the optimization effect on the lower nickel steel plate is not obvious due to the existence of fixed constraints that restrict pressure.

(4) The chosen material for the connecting structure in this article is nickel steel plates, which are widely used in the load-bearing connection structures of large and complex equipment and aerospace and other complex mechanical fields. By optimizing the structural layout, fatigue damage of bolt holes or plastic deformation of connectors caused by excessive hole perimeter stress can be effectively prevented. This enhances the safety, reliability and stability of load-bearing connection structures.

(5) This article studied the non-symmetrical triangular structure of bolt connections, providing an effective method and ideas for the layout optimization of non-symmetrical bolt configurations, enriching the research achievements in related fields.

This paper proves the correctness of applying algorithms to optimize bolt layouts. However, it only focuses on a specific equilateral triangular multi-bolt structure. In future studies, the layout optimization of randomly positioned multi-bolt structures should be further analyzed. Moreover, this article only conducts simulations on nickel steel plates, and subsequent experiments and simulations should cover different metal materials to enhance the applicability of this article.

Author Contributions: X.L. conducted experiments, data collection and analysis, and study design. M.Z. designed and conceived the project. Y.L. wrote and edited the manuscript to verify the correctness of the method. S.W. reviewed and edited the manuscript. Z.X. and S.L. investigated the research background and conducted a literature search. All authors have read and agreed to the published version of the manuscript.

Funding: This research received no external funding.

Institutional Review Board Statement: Not applicable.

Informed Consent Statement: Not applicable.

Data Availability Statement: Data sharing is not applicable to this article.

Conflicts of Interest: The authors declare that they have no conflict of interest.

References

1. Zhao, W.Y.; Yang, J.P.; Dong, X.H.; Huang, B. Simulation Analysis and Research of Deep Loosening Machine Shovel Seat Based on ANSYS Workbench. *South China Agric. Mach.* **2023**, *54*, 10–14.
2. Zhao, L.; Cai, H.; Wang, Z.Q.; He, J.J.; Wang, P.; Wang, B.; Qin, C.P.; Wang, B.H. Phased Array Ultrasonic Detection Method for Bolt Holes of Two In-service Fans. *Therm. Power Gener.* **2023**, *52*, 67–72.
3. Wang, X.T. *Study on Stiffness and Strength of Single Lap Bolted Joint Plate under Shear Load*; Nanchang Hangkong University: Nanchang, China, 2021.
4. Huang, L. Numerical Study on Optimal Geometric Parameters for Multi-performance of Friction High-Strength Bolts. *Int. J. Steel Struct.* **2022**, *22*, 56–69. [CrossRef]
5. Liu, C.; Zhou, Z.G.; Fang, B.H.; Hu, S.J.; Zhang, B. Experimental study on Mechanical properties of unsymmetrical reaming bolted Connection. *Eng. Seism. Resist. Reinf.* **2022**, *44*, 37–44.
6. Wu, S.J.; Liu, W.G. Research on Optimal Anti-Resonance Layout of Bolted Plate. *Mach. Tool Hydraul.* **2020**, *48*, 164–168.
7. Pedersen, N.L. Overall bolt stress optimization. *J. Strain Anal. Eng. Des.* **2013**, *48*, 155–165. [CrossRef]

8. Shen, B.; Pan, Z.W.; Lin, H.; Li, W.Z. Bolt layout optimization design based on genetic algo-rithm. *IOP Conf. Ser. Mater. Sci. Eng.* **2019**, *576*, 012005. [CrossRef]
9. Han, J.G.; Wu, Z.; Sun, Y.L.; Zhang, W.Q. Multi-joint integrated Motion trajectory Optimization of Robot based on Gray Wolf Algorithm. *J. Nav. Univ. Eng.* **2020**, *32*, 90–95.
10. Liang, Y.F.; Xu, J.G.; Wu, M. GPS Fast clock difference prediction Method Optimized by Elman Neural Network based on Particle swarm Optimization Algorithm. *J. Nav. Univ. Eng.* **2022**, *34*, 41–47.
11. Wang, C.F.; Zhou, H.L. Optimization of Bolt Connection Structure Layout Based on Firefly Algorithm. *Mach. Tool Hydraul.* **2022**, *50*, 144–147.
12. Kwon, Y.D.; Lee, D.S. A study on design optimization of conical bolt in the tf coil structure of the kstar tokamak. *Int. J. Mod. Phys. B* **2008**, *20*, 4475–4480. [CrossRef]
13. Lalaina, R.; Jeet, D.; Patrick, O.; Grégoire, A. Coupled topology optimization of structure and connections for bolted mechanical systems. *Eur. J. Mech. A/Solids* **2022**, *93*, 104499.
14. Kim, M.; Kim, Y.; Kim, P.; Park, J. Design Optimization of Double-array Bolted Joints in Cylindrical Composite Structures. *Int. J. Aeronaut. Space Sci.* **2016**, *17*, 332–340. [CrossRef]
15. Zhao, S.; Li, D.; Xiang, J. Multi-objective optimum of composite bolted joints by using the multi-layer convex hull method. *Struct. Multidiscip. Optim.* **2018**, *58*, 1233–1242. [CrossRef]
16. Elik, L.D.; Ciftci, M.; Ozturk, Y. Effects of the external tendons on the system capacity and stud behavior in composite beams. *Structures* **2020**, *24*, 851–863.
17. Pan, W.C. Application of Fruit Fly optimization Algorithm to optimize generalized regression neural network for enterprise performance evaluation. *J. Taiyuan Univ. Technol.* **2011**, *29*, 1–5.
18. Poli, R.; Kennedy, J.; Blackwell, T. Particle swarm optimization. *Swarm Intell.* **2007**, *1*, 33–57. [CrossRef]
19. Mirjalili, S.; Mirjalili, M.S.; Lewis, A. Grey Wolf Optimizer. *Adv. Eng. Softw.* **2014**, *69*, 46–61. [CrossRef]
20. Mirjalili, S.; Mirjalili, M.S.; Hatamlou, A. Multi-Verse Optimizer: A nature-inspired algorithm for global optimization. *Neural Comput. Appl.* **2016**, *27*, 495–513. [CrossRef]
21. Zikri, B.; Muge, K.; Jeremy, A.B.; Douglas, H. The Wind Driven Optimization Technique and its Application in Electromagnetics. *IEEE Trans. Antennas Propag.* **2013**, *61*, 2745–2757.
22. Pan, C.S.; Si, Z.H.; Xi, L.; Lv, Y.N. A four-step decision-making grey wolf optimization algorithm. *Soft Comput.* **2021**, *25*, 14375–14391. [CrossRef]
23. Yu, X.W.; Huang, L.P.; Liu, Y.; Zhang, K.; Li, P.; Li, Y. WSN node location based on beetle antennae search to improve the Gray wolf algorithm. *Wirel. Netw.* **2022**, *28*, 539–549. [CrossRef]
24. Chen, B.C.; Lv, Z.M. Finite Element Analysis of Sealing Contact Based on Abaqus Gasket. *China Water Transp. (Second Half)* **2023**, *23*, 62–64.
25. He, H.B. Optimization Design of Bolted Steel Member Based on Genetic Algorithm. *Comput. Appl. Softw.* **2011**, *28*, 236–238.
26. Beijing Iron and Steel Design Research Institute. *Steel Structure Design Code GB 50017-2017 [S]*; China Building and Construction Press: Beijing, China, 2017.
27. *GB/T197-2003*; The General Administration of Quality Supervision, Inspection and Quarantine of the People's Republic of China and the Standardization Administration of China. Standards Press of China: Beijing, China, 2003.
28. Liao, R.; Sun, Y.; Liu, J.; Zhang, W. Applicability of damage models for failure analysis of threaded bolts. *Eng. Fract. Mech.* **2011**, *78*, 514–524. [CrossRef]
29. Yang, G.; Yang, L.; Chen, J.; Xiao, S.; Jiang, S. Competitive Failure of Bolt Loosening and Fatigue under Different Preloads. *Chin. J. Mech. Eng.* **2021**, *34*, 1–11. [CrossRef]
30. Xiao, L.J.; Gong, X.B.; Zhu, X.L.; Chi, Y.R. Optimal design of mining explosion-proof box bolt set layout. *Coal Eng.* **2016**, *7*, 129–131.
31. Xiao, W.Y.; He, E.M.; Hu, Y.Q. A new method for optimizing the bolt layout of connectors based on improved genetic algorithm. *J. Northwest. Polytech. Univ.* **2017**, *35*, 414–421.
32. Wang, C.F. *Mechanical Analysis and Layout Optimization Design of Bolted Connection Structure*; Hefei University of Technology: Hefei, China, 2021.